

DOI: 10.1002/cbic.201300359

VIP

Chemical and Structural Insights into the Regioversatility of the Aminoglycoside Acetyltransferase Eis

Jacob L. Houghton,^[a, c] Tapan Biswas,^[a] Wenjing Chen,^[b, c] Oleg V. Tsodikov,^{*, [d]} and Sylvie Garneau-Tsodikova^{*, [d]}

A recently discovered cause of tuberculosis resistance to a drug of last resort, the aminoglycoside kanamycin, results from modification of this drug by the enhanced intracellular survival (Eis) protein. Eis is a structurally and functionally unique acetyltransferase with an unusual capability of acetylating aminoglycosides at multiple positions. The extent of this regioversatility and its defining protein features are unclear. Herein, we determined the positions and order of acetylation of five aminoglycosides by NMR spectroscopy. This analysis revealed unprece-

ented acetylation of the 3'-amine of kanamycin, amikacin, and tobramycin, and the γ -amine of the 4-amino-2-hydroxybutyryl group of amikacin. A crystal structure of Eis in complex with coenzyme A and tobramycin revealed how tobramycin can be accommodated in the Eis active site in two binding modes, consistent with its diacetylation. These studies, describing chemical and structural details of acetylation, will guide future efforts towards designing aminoglycosides and Eis inhibitors to overcome resistance in tuberculosis.

The emergence and spread of drug-resistant bacteria pose a great global health threat, as they are outpacing the development of novel antibiotics. Prominent examples are multidrug-resistant (MDR) and extensively drug-resistant (XDR) strains of *Mycobacterium tuberculosis* (*Mtb*) that cause highly lethal tuberculosis (TB). The aminoglycoside (AG) kanamycin (Kan) is often chosen as a drug of last resort to treat such infections. It was recently discovered that upregulation of the enhanced intracellular survival (*eis*) gene was the sole cause of resistance to Kan in one-third of a large and diverse set of *Mtb* clinical isolates.^[1] Most recently, specific mutations in the *eis* gene in XDR-*Mtb* strains were found to be strongly associated with resistance to all AGs and to the amine-rich peptide capreomycin, another drug used in MDR-TB and XDR-TB therapy.^[2] The *eis* gene encodes the acetyltransferase Eis, and the increased acetylation of Kan upon upregulation of *eis* causes the resistance,^[1a] as the acetylated Kan cannot bind to its target, the ribosome. We previously demonstrated that, unlike other known AG acetyltransferases (AACs), all of which regiospecifically acetylate a single position on any given AG, Eis from *Mtb* and its homologues

from other bacteria^[3] can efficiently transfer the acetyl group from acetyl coenzyme A (AcCoA) to multiple amine functionalities on a variety of lysine-containing peptides, including capreomycin,^[4] and AG scaffolds, including Kan and amikacin (Amk).^[5] Eis is also unique structurally; it is a hexamer, with each monomer composed of three fused domains: the N-terminal GNAT domain, which bears most of the residues directly involved in AcCoA binding and catalysis of acetyl transfer, the central cyclically permuted GNAT domain that, together with the N-terminal GNAT domain, forms an intricate AG binding pocket, and the C-terminal domain, with a sterol binding protein fold that performs the scaffolding role and positions the C-terminal carboxy group in the active site to serve as a general base in acetyl transfer. Despite this progress, the mechanistic picture of the intriguing multi-acetylation capability of Eis has remained unclear. In this study, we carried out a detailed investigation of the specificity and order of multi-acetylation of five clinically relevant AGs by Eis from *Mtb* by using a combination of thin-layer chromatography (TLC) and nuclear magnetic resonance (NMR) spectroscopy. We discovered acetylation at positions that are not modified by any other known AAC. In addition, we determined the crystal structure of a ternary complex of Eis with coenzyme A (CoA) and one of the AGs, tobramycin (Tob), to characterize the substrate binding features, which revealed two possible binding modes of this AG in the Eis active site, consistent with the two positions acetylated on Tob.

Results and Discussion

Analysis of positions and the order of acetylation of AGs by Eis from *Mtb*

Eis is unique among all AACs in exhibiting regioversatility; it efficiently acetylates several AGs at multiple amine positions.^[5] Other known AACs are strictly regiospecific and are divided into classes based on the sites that they acetylate. AAC(6'),


[a] Dr. J. L. Houghton,⁺ Dr. T. Biswas⁺
Department of Medicinal Chemistry, University of Michigan
Ann Arbor, MI 48109 (USA)

[b] Dr. W. Chen
Chemical Biology Doctoral Program, University of Michigan
Ann Arbor, MI 48109 (USA)

[c] Dr. J. L. Houghton,⁺ Dr. W. Chen
Life Sciences Institute, University of Michigan
Ann Arbor, MI 48109 (USA)

[d] Dr. O. V. Tsodikov, Dr. S. Garneau-Tsodikova
Department of Pharmaceutical Sciences, University of Kentucky
Lexington, KY, 40536-0596 (USA)
E-mail: sylviegsodikova@uky.edu
oleg.tsodikov@uky.edu

[⁺] These two authors contributed equally to this work.

 Supporting information for this article is available on the WWW under <http://dx.doi.org/10.1002/cbic.201300359>.

AAC(2'), AAC(3), and AAC(1) have been reported, and representatives of AAC(6'), AAC(2'), AAC(3) were used in this study to obtain acetylated AGs to be used as standards. TLC was used to study AG acetylation, as the retention factor (R_f) of AGs changes upon acetylation. We compared the R_f values for Eis-modified Amk, Kan, sisomicin (Sis), netilmicin (Net), and Tob to the respective 6'-, 2'-, and 3-mono-acetylated counterparts, and, when possible, to their 6',2'-, 6',3'-, and 3,2'-diacetylated counterparts (Table 1). The diacetylated standards were obtained by sequential acetylation with the selective AACs as previously described.^[5,6]

Previous studies indicated that Kan and Amk were readily diacetylated by Eis, and that the 4-amino-2-hydroxybutyryl (AHB)-containing Amk could be triacetylated to some extent, as determined by liquid chromatography-mass spectrometry (LCMS), but the positions and the order of acetylation were not established.^[5] Following the reaction progress by TLC and LCMS revealed that Kan underwent two acetylations relatively rapidly, and the modifications did not follow a strict order (Figure 1 and Table 1, Figure S1 and Table S1). The R_f value of the diacetylated Kan product of Eis did not match that of any acetylated standards, thus indicating at least one position to be novel. The diacetylated product from a scaled-up reaction was purified by silica gel flash chromatography for NMR analysis (Tables S2-3, Figure S2-11). A comparison of the 1D and 2D ¹H and ¹³C NMR spectra of Kan to the diacetylated Kan product clearly indicated that the reactions occurred at the 6'- and 3''-amines. This is the first report of acetylation at the 3''-position of any AG by an AAC.

TLC analysis of the acetylation of Amk by Eis indicated that as many as three acetylated products could be formed and that, similarly to Kan, their formation did not follow a strict order (Figure 1 and Table 1). Among the regiospecific AAC en-

zymes mentioned earlier, Amk is a good substrate only for AAC(6'), which limits available standards and thereby limits the utility of TLC in determining the Eis regiospecificity for this AG. Of the three products formed by Eis that were resolved by TLC, the one with the lowest R_f value closely matched that of 6'-acetyl-Amk. The reaction was scaled up and purified by silica gel flash chromatography for 1D and 2D ¹H NMR analysis (Table S4, Figures 2 and S12-18). NMR analysis revealed that the dominant ultimate product with an R_f value of 0.46 was an Amk that was diacetylated similarly to Kan, but, to our surprise, in this case the reactions had occurred at the 3''-position and the γ -amine of the AHB moiety. This is the first report of an AAC capable of modifying the AHB moiety of Amk. It is important to note that for Amk, Net, Sis, and Tob, NMR experiments were performed in 10% D₂O, which provided two means of determining the exact positions acetylated: 1) visualization of amide proton coupling in 2D spectra, and 2) chemical shift patterns.

In contrast to Amk and Kan, for which multiple acetylations followed a random order, TLC analysis of the time course of acetylation of Sis and Net by Eis showed that the reactions proceeded in an ordered sequential manner, with the second acetylation occurring significantly more slowly than that observed for Kan or Amk (Figure 3 and Table 1). For both Sis and Net, TLC indicated that Eis specifically and rapidly acetylated a single amine, and a comparison with the standards strongly suggested that the amine at the 6'-position was acetylated. For Net, the first acetylation was followed by a single second acetylation, and for Sis, by two slow acetylations. In order to determine the order of acetylation, we modified our method to monitor reaction progress by NMR without the need for time-consuming chromatographic separation and purification of the products. AcCoA was added in a stepwise fashion over

Table 1. R_f values^[a] of mono- and diacetylated AGs by the AAC(2')-Ic, AAC(3)-IV, AAC(6'), and Eis proteins.

AG		Enzymes utilized							Eis					
		None	(2') ^[e]	(3) ^[f]	(6') ^[g]	(3)/(2')	(6')/(2')	(6')/(3)	1 min	5 min	10 min	30 min	2 h	O/N
Amk	parent ^[b]	0.06							0.06	0.06	0.06	0.06		
	mono ^[c] di ^[d]		× ^[h]	× ^[i]	0.10			× ^[i]		0.10/0.36	0.10/0.36	0.10/0.36	0.10/0.36	0.46
Kan	parent	0.28							0.28					
	mono di		× ^[h]	0.33	0.43			× ^[h]	0.49	0.33	0.33/0.43	0.33/0.43	0.33	0.56
Net	parent	0.06								× ^[j]	× ^[j]	× ^[j]		× ^[j]
	mono di		× ^[j]	× ^[j]	0.26			– ^[k]	0.37			0.26		
Sis	parent	0.05												
	mono di		0.08	0.16	0.24					0.24	0.24	0.24	0.24	0.24
Tob	parent	0.24								0.24	0.24			
	mono di		0.27	0.36	0.48			– ^[k]	– ^[k]	0.48	0.29/0.48	0.48	0.48	0.62

[a] The eluent systems used for TLC were MeOH/NH₄OH (5:2 for Amk, Kan, and Tob; 25:1 for Net; and 15:2 for Sis). [b] Parent indicates no acetylation. [c] Mono indicates monoacetylation. [d] Di indicates diacetylation. [e] (2') indicates AAC(2')-Ic. [f] (3) indicates AAC(3)-IV. [g] (6') indicates AAC(6') of the AAC(6')/APH(2''). [h] Because the 2'-NH₂ does not exist in Amk or Kan, these controls were not performed. [i] Amk is not a substrate for AAC(3)-IV. [j] These reactions were not performed. [k] Indicates that the diacetylated product could not be visualized as it had an R_f value overlapping with that of the glycerol in the reaction mixture, as the sequential use of enzymes did not work in these cases. [l] Based on NMR analysis, this most likely corresponds to the 3''-acetyl-Tob.

AGs acetylated in a random order by Eis:

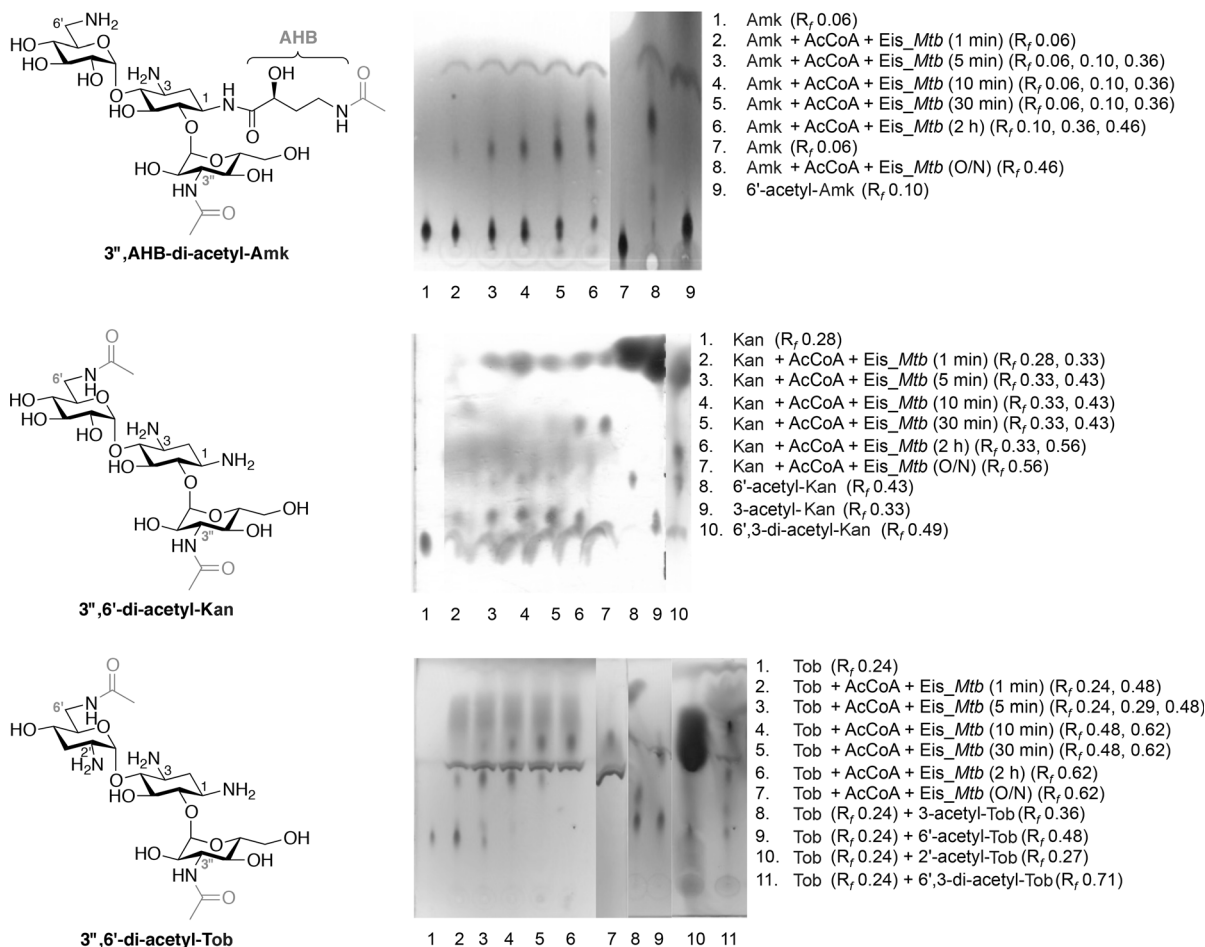


Figure 1. AGs acetylated in random order by Eis. Top: Diacetylation of AMK by Eis observed by TLC. Lanes 1 and 7: Amk. Lanes 2–6 and 8: time course displaying the mono- and diacetyl-Amk products of the Eis reaction. Lane 9: control for 6'-acetylation of Amk performed with AAC(6'). Middle: Diacetylation of Kan by Eis observed by TLC. Lanes 1–7: time course displaying the mono- and diacetyl-Kan products of the Eis reaction. Lanes 8–10: controls for the mono- and diacetylation of Kan performed with AAC(6') and AAC(3)-IV individually or sequentially. Bottom: Diacetylation of Tob by Eis observed by TLC. Lanes 1–7: time course displaying the mono- and diacetyl-Tob products of the Eis reaction. Lanes 8–11: controls for the mono- and diacetylation of Kan performed with AAC(6'), AAC(3)-IV, and AAC(2)-Ic individually or sequentially.

the course of the reaction to control the reaction progress and facilitate identification of monoacetylated species. NMR analysis of a reaction mixture containing a 1:1 molar ratio of AcCoA and Net showed rapid and complete conversion to the 6'-acetylated product, as suggested by TLC (Table S5, Figure S19–24). Addition of a second equivalent of AcCoA yielded a single diacetylated product. This second sequential acetylation occurred at the 2'-amine to give the 6',2'-diacetyl-Net product (Table S6, Figure S19–21 and S25–27).

For Sis, NMR analysis was carried out in a similar fashion. At a 1:1 molar ratio of AcCoA and Sis, complete conversion to 6'-acetyl-Sis was observed (Table S7, Figure S28–36). The R_f values of the two additional Eis acetylated Sis products were similar to two diacetylated Sis standards, 6',2'- and 6',3'-diacetyl-Sis. These products formed much more slowly than in the previous cases and required addition of four equivalents of AcCoA and prolonged overnight incubation to drive the reaction to completion from 6'-acetyl-Sis. A mixture of the two products was purified by flash chromatography for further NMR experiments

(Table S8, Figure S28–33 and S37–42). The relatively small difference in R_f values precluded complete separation of these two products; therefore, NMR analysis was carried out on a mixture of these two compounds. The analysis indicated that Sis was converted into two distinct diacetylated products, and that a triacetylated product was formed in amounts insufficient for its characterization. One of the products was unambiguously determined to be 6',2'-diacetyl-Sis (Figure 3). The second diacetylated product contained an acetyl group in ring II at either the 1- or 3-position; the exact position could not be assigned with certainty, as the amine at these two positions overlap in NMR spectra and cannot be differentiated by 2D NMR due to the pseudo-symmetrical substitution of ring II.

We further performed similar experiments on Tob because it contains a different pattern of functionalities in ring I, and is otherwise identical to Kan. Previous LCMS analysis showed that Tob can be acetylated by Eis at as many as four positions.^[5] TLC characterization and mass spectrometry experiments indicated that two dominant acetylations occurred and

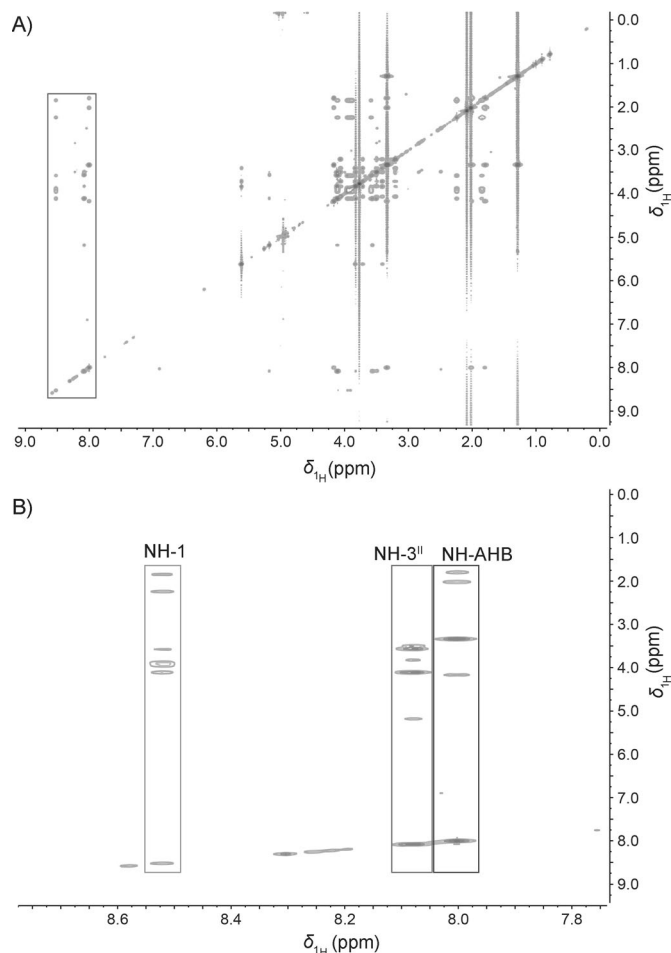
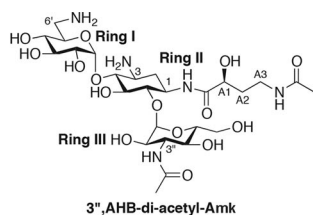


Figure 2. A representative zTOCSY spectrum recorded at 600 MHz in H₂O/D₂O (9:1) showing the 3'',AHB-diacetyl-Amk. The full spectrum is shown in panel A, and the expansion showing the amide protons coupled to the protons at the 1-, 3'', and AHB-positions in panel B. The box in panel A indicates the portion of the spectrum expanded and shown in panel B. In panel B, coupling of the amide protons at the 1-, 3'', and A3 of the AHB positions are indicated by boxes with different shades of gray.

that they were not strictly ordered, as with Kan and Amk (Figures 1 and S1, Tables 1 and S1). Comparison with acetylated Tob standards indicated that one of the first acetylations likely occurred at the 6'-amine, whereas the other mono-acetylated product did not match any of the standards. NMR analysis of the reaction containing a 1:1 molar ratio of Tob and AcCoA indicated that the two monoacetylated products formed in an approximately 6:4 ratio. Addition of another equivalent of AcCoA resulted in the complete conversion of Tob to a single 6',3''-diacetylated product (Table S9, Figure S43–48), demonstrating the same regioselectivity of Eis towards Tob and Kan.

Effect of acetylation of Amk, Kan, Net, Sis, and Tob by Eis on the antibiotic activity of these AGs

Both Kan and Amk are inactivated upon Eis acetylation, as previously demonstrated by bio-TLC assays.^[1a] We tested the effect of multiple acetylations of the AGs by Eis on their antibiotic activity against *Escherichia coli* and *Mycobacterium smegmatis* in disc diffusion assays. These experiments demonstrate that all five AGs: Amk, Kan, Net, Sis, and Tob, lose their antibiotic activity against *E. coli* and *M. smegmatis* upon multiacetylation by Eis (Figure 4).

Crystal structure of Eis in complex with CoA and Tob

Capturing a stably bound AG in the active site of Eis in crystals has been a significant challenge. This is likely, at least in part, due to binding of the AG in multiple orientations in the Eis active site to position different amines for acetylation. Previous co-crystallization experiments of Eis, Eis-CoA, and Eis-AcCoA with several AGs did not reveal a clear electron density for an AG.^[5] Soaking these crystals with a variety of AGs also did not yield a structure with a bound AG. We observed that, in addition to one CoA molecule bound at its cognate site (essential for Eis crystal formation), another CoA formed a disulfide bond to the thiol of Cys204 upon oxidation over the long crystallization times needed for crystal growth, as evidenced by the presence of partial electron density for this CoA adduct in some electron density maps. Because Cys204 is located close to the entry of the AG binding pocket, this spurious CoA adduct formation might obstruct or partially occlude binding of an AG, thus destabilizing its Eis-bound state. To remove this artifact of long incubation, we generated the EisC204A mutant. This mutant displayed similar acetylation efficiency to that of wild-type Eis for several AGs (Figure S49). A crystal structure with an AG bound to Eis was obtained from crystals of an EisC204A-CoA-Tob complex and refined at 3.5 Å resolution (Table 2). Two of the six AG binding pockets of the Eis hexamer contained strong and continuous difference electron density corresponding to the bound Tob (Figure 5). This electron density did not have a sharply delineated boundary, possibly due to resolution limitations or due to Tob binding to the Eis active site pocket in two or more binding modes, each partially occupied in the crystal. A Tob molecule could be refined in either one of two possible binding modes, approximately related to each other by a 180° rotation, a shift and a minor conformational change (Figure 5C, D). These two binding modes are consistent with the two dominant acetylations of Tob, one at the 6'-position (Figure 5C) and the other at the 3''-position (Figure 5D). Moreover, both the conformation and position of Tob in the active site consistent with 6'-acetylation closely resemble those in the crystal structure of AAC(6')-Ig from *Acinetobacter haemolyticus* in complex with Tob (PDB code: 4EVY). As previously predicted, the Tob-interacting residues are located in all three regions of Eis.^[5] In either conformation, Tob is held in the binding pocket by several direct electrostatic and hydrogen bonding interactions between the amine and hydroxy groups of the Tob with protein carboxylates (Asp26,

AGs acetylated in a strict order by Eis:

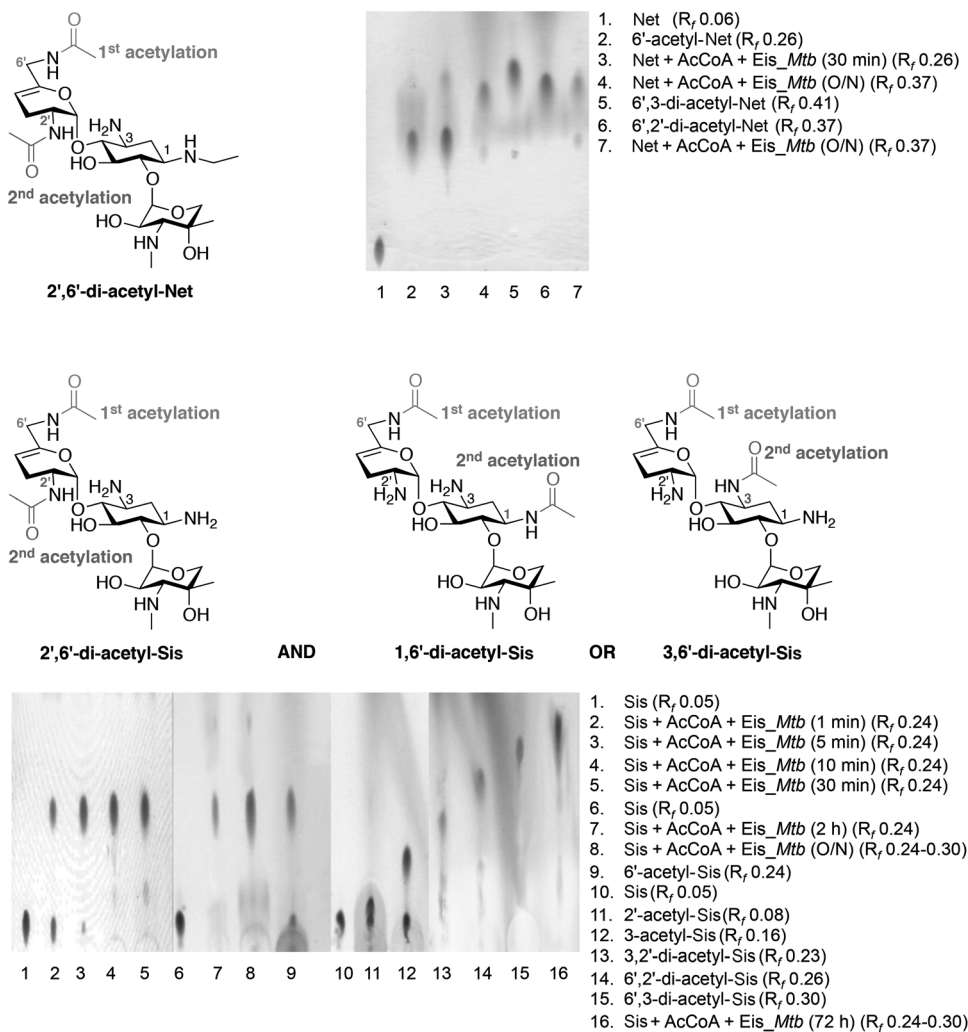


Figure 3. AGs acetylated in strict order by Eis. Top: Diacetylation of Net by Eis observed by TLC. Lanes 1, 3, 4, and 7: time course displaying the mono- and diacetyl-Net products of the Eis reaction. Lanes 2, 5, and 6: controls for the mono- and diacetylation of Net performed with AAC(6'), AAC(3)-IV, and AAC(2')-Ic individually or sequentially. Bottom: Diacetylation of Sis by Eis observed by TLC. Lanes 1–8 and 16: time course displaying the mono- and diacetyl-Sis products of the Eis reaction. Lanes 9 and 11–15: controls for the mono- and diacetylation of Net performed with AAC(6'), AAC(3)-IV, and AAC(2')-Ic individually or sequentially.

Glu203, Glu401, and the C-terminal carboxy group). In addition, the Tob molecule is cradled by nonpolar contacts between its rings and the nonpolar side chains (Ile28, Trp36, Phe24, and Phe84). Specifically, the modified sugar ring is oriented by contacts with Phe24 and Phe84, and the ring distal from the modification site makes hydrophobic contacts with Ile28 and Trp36. Stacking of sugar rings against aromatic residues or RNA bases appears to be a general mode of interaction seen in other crystal structures in which Tob is a ligand.^[7] The unique pocket structure of Eis among AG-modifying enzymes results in the unique nature of its interactions with Tob in the following respects. A Tob molecule bound to Eis-CoA is highly protected from solvent, more so than in any other structurally characterized protein-Tob complex (Table S10). Solvent-accessible surface area analysis indicated that this extra desolvation is due to the nonpolar Tob-Eis interactions not seen in other protein-

Tob structures. In fact, nonpolar surface area buried in the Tob-Eis interface dominates buried polar surface area, in contrast to other protein-Tob complexes (Table S11). The larger contribution of nonpolar residues lining the AG binding pocket of Eis, compared with other AG-modifying enzymes, might explain the versatility of binding an AG in different conformations, as strict geometric constraints imposed by hydrogen bonds and electrostatic interactions, which generally dictate a particular orientation of a bound substrate, appear to play a relatively minor role in the case of Eis.

Conclusions

Herein we investigated the regioversatility of the AAC Eis and demonstrated that this enzyme is unique in its capability to acetylate the 3''-position of Amk, Kan, and Tob, as well as the γ -amine of the AHB group of Amk. Neither position is known to be modified by any other characterized AAC. Interestingly, a previous report implicated point mutant D80G of AAC(6')/APH(2'') from *Staphylococcus aureus* in arbekacin acetylation at the γ -amine of the AHB group,^[8] which was observed in bacterial extracts containing this mutant enzyme.^[9]

Similarly to inactivating acetylations by Eis and other AACs at other positions, these two newly discovered modifications are predicted to destabilize AG-ribosome binding, as these amines form hydrogen bonds with RNA bases in the decoding A-site of the ribosome.^[10] The acetyl groups at these positions might also disrupt other interactions, as the acetylated AG would not be accommodated sterically in the same bound conformation. Indeed, acetylation of all five AGs examined in this study by Eis abolished their antibiotic activity against both *E. coli* and *M. smegmatis*, confirming a similar observation made previously with Kan and Amk.^[1a] In addition to these unusual modifications, Eis can acetylate AGs at one or more of all possible positions (1, 2', 3, and 6') that were previously reported to be modified by other AACs.^[11] The multi-acetylation of AGs by Eis displays specificity, as not all the amines are modified on any AG studied to date, and similar AGs share some common modification positions.

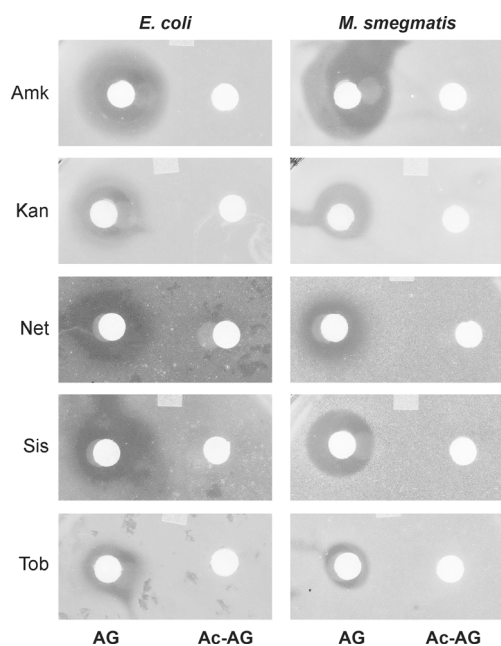


Figure 4. Disc diffusion assays demonstrating antibiotic activity of Kan, Amk, Net, Sis, and Tob against *E. coli* BL21 (DE3) and *M. smegmatis* MC2-155 (discs labeled "AG") and abrogation of this activity upon acetylation of these AGs by Eis (discs labeled "Ac-AG").

Table 2. X-ray diffraction data collection and refinement statistics for the EisC204A-CoA-Tob ternary complex structure.	
Data collection	
space group	$P2_1$
number of monomers per asymmetric unit	6
Unit cell dimensions	
a, b, c [Å]	82.2, 154.9, 115.3
α, β, γ [°]	90, 104.7, 90
resolution [Å]	50.0–3.5 (3.56–3.50) ^[a]
I/σ	14.9 (2.3)
completeness [%]	100.0 (99.7)
redundancy	3.8 (3.8)
R_{merge}	0.10 (0.64)
number of unique reflections	33 556
Structure refinement statistics	
resolution [Å]	40.0–3.5
R [%]	24.6
R_{free} [%]	27.6
bond length deviation (rmsd) from ideal [Å]	0.005
bond angle deviation (rmsd) from ideal [°]	1.100
Ramachandran plot statistics^[b]	
residues in most allowed regions [%]	92.1
residues in additional allowed regions [%]	7.9
residues in generously allowed regions [%]	0.0
residues in disallowed regions [%]	0.0 (0 residues)
[a] Numbers in parentheses indicate the values in the highest-resolution shell. [b] Indicates Procheck statistics. ^[22]	

Nevertheless, the regioversatility of Eis is truly remarkable, as the acetylation specificity pattern depends on a particular AG scaffold, as well as on the presence of modifications on the same scaffold. For example, the AHB group of Amk, which normally renders its unmodified analogue, Kan, inert towards modifications by some AG-modifying enzymes, switches Eis re-

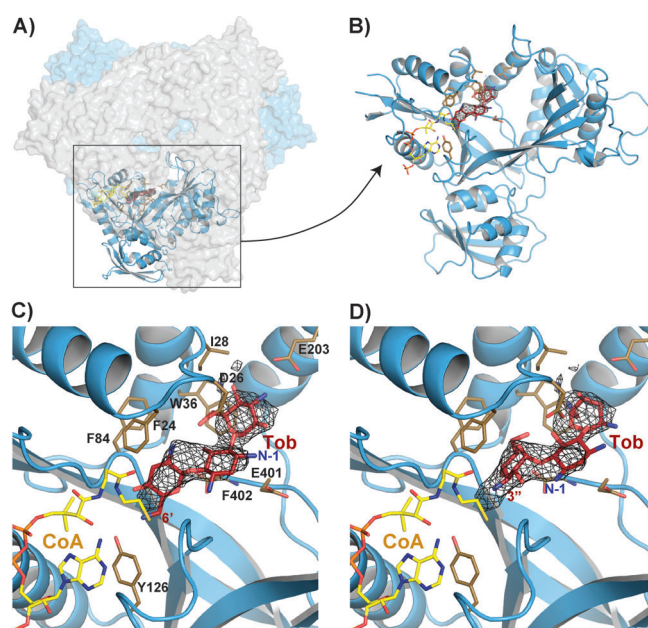


Figure 5. Crystal structure of the EisC204A-CoA-Tob complex. A) View of the Tob-containing active site in the EisC204A hexamer. B) The Tob-bound EisC204A monomer. C) Tob bound in the conformation consistent with 6'-acetylation. D) Tob bound in the conformation consistent with 3'-acetylation. The black mesh is the omit $F_o - F_c$ electron density map generated without Tob in the model and contoured at 3σ . CoA, Tob, and Tob-interacting residues of EisC204A are shown as yellow, red, and brown sticks, respectively. The positions of acetylation and the N-1 position are labeled in red and blue, respectively.

giospecificity from the 3'- and 6'-amines of Kan to the 3'- and AHB-amines of Amk. The large AHB adduct apparently disfavors binding of Amk for its modification at the 6'-amine and stabilizes an alternative bound conformation for acetylation of the AHB-amine. Analogously, acetylation by Eis itself can alter the binding mode of an AG to Eis, which explains the strictly ordered acetylation of Sis and Net. It is possible that a relatively high planarity of the unsaturated sugar rings of these two AGs strongly stabilizes Sis and Net in one preferred Eis-bound conformation, due to the π - π stacking of these rings with protein residues, similar to the π - π stacking of the unsaturated ring of 6'-hydroxy-Sis with the G1491 of decoding site RNA observed recently by X-ray crystallography.^[12] Acetylating these AGs at one position creates a new, less charged surface on these molecules, apparently making favorable new binding modes for further acetylations. For Amk, Kan, and Tob, there are at least two main orientations in which these AGs can bind Eis initially, each leading to acetylation, as evidenced by a random order of their acetylation.

The crystal structure of the ternary EisC204A-CoA-Tob complex reveals the two possible binding modes of Tob that would lead to its observed 3'',6'-diacetylation. The structure clearly shows a large contribution of nonpolar contacts of the AG to the binding interface, both in the absolute sense and relative to the nature of Tob contacts with other AG-modifying enzymes. As a dominant contribution to the nonpolar contacts is made by the interactions of Eis with the sugar scaffold of Tob, resulting in nearly complete dehydration of Tob, a particu-

lar binding mode of an AG, and hence its pattern of modification, is generally guided by its core scaffold. The large N-1-AHB group of Amk likely binds in the same binding channel with its amine positioned for acetylation. This group could sterically and electrostatically clash with Gly401 of Eis if Amk is positioned for its acetylation at the 6'-position, but not if Amk is positioned for its acetylation at the 3''-position, based on the respective Tob binding modes (Figure 5C, D). In addition, acetyl groups newly incorporated by Eis itself can alter binding modes of an AG, at least in part by nonpolar stabilizing contacts in the Eis substrate binding pocket, thereby positioning another amine for acetylation.

The versatile acetylation of AGs and peptides by Eis^[4] appears to be regulated in vivo, likely to avoid deleterious effects of such acetylation of metabolites and proteins. This regulation was reported to occur at the transcriptional level,^[13] no regulatory interacting partners of Eis are known. In fact, resistance to Kan arises due to upregulating mutations in the *eis* promoter.^[1a] The highly versatile AG multi-acetylation function of Eis is alarming in terms of the evolution of antibiotic resistance. Together with the lack of effective treatments for TB, the increasing number and severity of outbreaks of MDR- and XDR-TB underscores an urgent need for discovery of novel drugs. The development of novel synthetically modified AGs that avoid resistance enzymes, reduce toxicity, and improve efficacy has been the goal of numerous research efforts. However, the combined versatility and promiscuity of Eis poses a hindrance to the development of new AGs for TB treatment, particularly because of the modification potential of Eis towards the AHB moiety, which has been shown to improve resistance properties of many AGs when incorporated at the N-1 position. Therefore, an alternative course of action might be necessary to overcome TB resistance to AGs. One such approach is the development of Eis inhibitors to be used in combination with AGs against AG-resistant TB.^[14] This approach mirrors a time-tested β -lactam/ β -lactamase inhibitor combination therapy and the meropenem/clavulanate combination recently discovered to be effective against XDR-TB.^[15] The functional and structural studies of Eis presented here bring us one step closer to tackling the TB drug resistance problem.

Experimental Section

Materials and instrumentation: Eis,^[5] AAC(2')-Ic,^[5] AAC(3)-IV,^[6] and AAC(6')/APH(2'')^[6] were purified as before. NMR spectra were recorded on Bruker Avance III 600 MHz and Varian 400 and 500 MHz spectrometers. LCMS was performed on a Shimadzu LCMS-2019EV.

TLC: TLC plates were stained with cerium molybdate.^[5] The eluents were MeOH/NH₄OH (5:2 for Amk, Kan, Tob; 25:1 for Net; and 15:2 for Sis; Table 1).

TLC of monoacetylated AG standards: Reactions (15 μ L) were performed in MES (50 mM, pH 6.6) for AAC(3)-IV and AAC(6') or in Na₂HPO₄ (100 mM, pH 7.0) for AAC(2')-Ic with AcCoA (0.96 mM), AG (0.8 mM), and AAC (10 μ M). After overnight incubation at room temperature, an aliquot (5 μ L) was loaded onto a TLC plate and eluted.

TLC of diacetylated AG standards: Diacetylation reactions were carried out with AAC(6') followed by AAC(2')-Ic, AAC(3)-IV followed by AAC(2')-Ic, or AAC(6') followed by AAC(3)-IV. Reactions (10 μ L) were performed in MES (50 mM, pH 6.6) with AcCoA (1.92 mM), AG (0.8 mM), and the first AAC (10 μ M). After overnight incubation at room temperature, the second AAC (10 μ M) was added, and the reaction proceeded for > 16 h. An aliquot of each reaction (5 μ L) was loaded onto a TLC plate and eluted.

TLC of AGs multi-acetylated by Eis: Reactions (30 μ L) were performed in Tris-HCl (50 mM, pH 8.0) with AcCoA (4 mM), AGs (0.8 mM), and Eis (5 μ M). Aliquots (4 μ L) were loaded onto a TLC plate after 0, 1, 5, 10, 30, 120 min, and more than 16 h at room temperature and eluted.

LCMS of multi-acetylated AG products: Masses were obtained in positive-ion mode using H₂O and 0.1% formic acid after dilution of the NMR samples described below (1 μ L of 15 mM stock) with H₂O (1 mL) and injection of 20 μ L of each product (Table S1, Figure S1).

NMR analysis of 3'',AHB-diacetyl-Amk: A reaction mixture (4 mL) containing Amk (5 mM), AcCoA (20 mM), and Eis (0.5 mg mL⁻¹) in Na₂HPO₄ (50 mM, pH 8.0) was incubated with shaking (room temperature, 24 h) prior to adding extra AcCoA (5 mM), adjusting the pH to 8.0 with 1.0 M KOH, adding Eis (0.1 mg mL⁻¹), and incubating for 48 h. After > 90% conversion of Amk into diacetyl-Amk, as judged by TLC, Eis was removed by MeOH precipitation. The supernatant was evaporated, and the residue was purified by SiO₂ flash chromatography using 0.0–2.0% Et₃N in MeOH. Fractions with product were pooled and concentrated under reduced pressure. The residue was dissolved in D₂O (minimal volume), adjusted to pH 3 with sulfuric acid (0.5%), and lyophilized. 3'',AHB-diacetyl-Amk (white powder) was dissolved in D₂O (400 μ L), centrifuged, and the supernatant collected for NMR analyses. The acetylated positions and purity were confirmed by ¹H, zTOCSY, and gCOSY NMR and LCMS. Proton connectivity was assigned using zTOCSY and gCOSY spectra. The NMR spectra of diacetylated-Amk (Figure S15–18) were compared to those of a non-acetylated Amk standard (Figure S12–14), prepared similarly to 3'',AHB-diacetyl-Amk (Table S4). Additionally, the compound was prepared in H₂O/D₂O (9:1), and ¹H and zTOCSY spectra were acquired.

NMR analysis of 3'',6'-diacetyl-Kan: Kan was diacetylated, and the product (white powder) was purified analogously to 3'',AHB-diacetyl-Amk. The acetylated positions and purity were confirmed by ¹H, ¹³C, gCOSY, gHMBC, and gHSQC NMR and LCMS. Proton connectivity was assigned using ¹H, zTOCSY, and gCOSY spectra. The signals of all carbons were assigned by using ¹³C, gHSQC, and gHMBC spectra. The NMR spectra of the diacetylated-Kan (Figure S7–11) were compared to those of a non-acetylated Kan standard (Figure S2–6), prepared similarly to 3'',6'-diacetyl-Kan (Tables S2–3).

NMR analysis of 2',6'-diacetyl-Net: The reaction was monitored by NMR without purification. To determine which modification occurred first, a reaction (400 μ L) containing Net (15 mM), AcCoA (15 mM), and Eis (0.5 mg mL⁻¹) in Na₂HPO₄ (25 mM, pH 8.0) containing 10% D₂O proceeded to > 90% completion. ¹H, gCOSY, and zTOCSY NMR experiments were performed with PURGE solvent suppression.^[16] After the first acetylation was complete and all spectra were acquired, AcCoA and Eis in 10% D₂O were added to yield a solution (600 μ L) containing Net (10 mM), AcCoA (20 mM), and Eis (0.1 mg mL⁻¹) in Na₂HPO₄ (25 mM, pH 8.0) containing 10% D₂O. Additional spectra were acquired after 48 h to determine the second site of acetylation. The acetylated positions, purity, and proton connectivity were analyzed as for Amk. The NMR spectra were compared to those of a Net standard [15 mM in Na₂HPO₄

(25 mM, pH 8.0) containing 10% D₂O] prepared identically to the reaction mixture without AcCoA and Eis (Tables S5–6). Representative spectra for 6'-acetyl-Net, 2',6'-diacetyl-Net, and Net are provided in Figure S22–24, S25–27, and S19–21, respectively.

NMR analysis of 2',6'- and 1/3,6'-diacetyl-Sis products: To determine the first position acetylated on Sis, the reaction was carried out as described for Net by using ~0.05 mg mL⁻¹ of Eis. After the first acetylation was complete and all spectra were acquired, aliquots of AcCoA (total of 4 equiv) were added, and spectra were acquired after incubating for 48 h to determine the subsequent sites of acetylation. Due to the complexity of the spectra, the final mixture of diacetylated products was purified for further analysis. After >90% conversion of Sis into two distinct diacetyl-Sis products, the products (white powder) were purified analogously to 3'',AHB-diacetyl-Amk. For NMR analyses, the mixture of products was dissolved in H₂O:D₂O (9:1, 400 μL), yielding a solution at pH 8 which was centrifuged and the supernatant collected. However, the acquired spectra were insufficient to fully characterize the compounds. The pH was adjusted to 3 with sulfuric acid (0.5%) for further analysis of the two diacetylated products. The acetylated positions, purity, and proton connectivity were analyzed as for Amk. Representative spectra for 6'-acetyl-Sis and the mixture of 2',6'-diacetyl-Sis and 1/3,6'-diacetyl-Sis are provided in Figure S34–36 and S37–42, respectively. The NMR spectra were compared to those of Sis standards at pH 3 and pH 8 prepared identically to the reaction mixture without Eis and AcCoA (Tables S7–8). Representative spectra of these standards are provided in Figure S31–33. Spectra of the standard at pH 8 in H₂O:D₂O (9:1) are provided in Figures S28–S30.

NMR analysis of 3'',6'-diacetyl-Tob: To determine the first position acetylated on Tob, the reaction (150 μL) was carried out as described for Net by using ~0.02 mg mL⁻¹ of Eis. After one equivalent of AcCoA was consumed, yielding a mixture of products (3''- and 6'-acetyl-Tob), and all spectra were acquired, another equivalent of AcCoA was added to form a single diacetylated product, 3'',6'-diacetyl-Tob, and spectra were acquired after incubating for 12 h. The NMR spectra were compared to those of a Tob standard [15 mM in Na₂HPO₄ (25 mM, pH 8.0) containing 10% D₂O], prepared identically to the reaction mixture without AcCoA and Eis (Table S9). Proton connectivity of 3'',6'-diacetyl-Tob was assigned by using zTOCSY and gCOSY spectra. Representative spectra for 3'',6'-diacetyl-Tob and the Tob standard are provided in Figures S46–S48 and S43–S45, respectively.

Disc diffusion assays of antibiotic activity of AGs before and after acetylation by Eis: *E. coli* BL21 (DE3) and *Mycobacterium smegmatis* MC2–155 cultures were grown on plates containing 20 mL of Luria-Bertani soft agar at 37 °C overnight. Acetylation reactions containing AG (Amk, Kan, Net, Sis, or Tob; 1 mM), AcCoA (5 mM), and Eis (5 μM) in Tris (50 mM, pH 8.0) were carried out to completion, as described above, with each AG. Twenty microliters of each reaction was spotted on a sterile filter paper disc (0.5 cm in diameter) and incubated at 37 °C overnight. On the same plates, 20 μL of each AG (1 mM) in the same buffer was spotted on paper discs. The antibiotic activity of all five AGs, as evidenced by the prominent zones of inhibition for the parent drugs, was abolished by the acetylation of the AGs by Eis (Figure 4).

Cloning, purification, and acetylation activity of EisC204A: EisC204A was constructed by splicing-by-overlap-extension.^[17] The sequences downstream and upstream of the mutation were individually amplified from pEis-pET28a(NHis) using primers #1:5'-CTGCTGGCAGAAgcgAAAGCCGCGCCCG-3' with #2:5'-CTAGCAG-

GATCCTCAGAACTCGAACGCG-3' and #3:5'-CCGCGGCATATGCTACAGTCGGATTC-3' with #4:5'-CGGGCGCGGCTTcgctTCTGCCAGCAG-3', respectively. These PCR products served as templates for another PCR with primers #2 and #3. This PCR product was subcloned into NdeI/BamHI-linearized pET28a. EisC204A was purified similarly to wild-type Eis,^[5] concentrated, and stored at 4 °C. The activity of EisC204A was tested against ten AGs by a UV/Vis assay^[5] (Figure S49).

Crystal structure determination of EisC204A-CoA-Tob complex: Crystals of the EisC204A-CoA-Tob complex were grown in hanging drops (22 °C, 2 months) consisting of a mixture of EisC204A (1 μL, 3.5 mg mL⁻¹) in Tris-HCl (50 mM, pH 8.0, containing Tob (1 mM) and CoA (1 mM) and reservoir solution (1 μL, Tris-HCl (100 mM, pH 8.5) and PEG 8,000 (13%, w/v)), equilibrated against 1 mL of reservoir solution. The crystals were gradually transferred into cryoprotectant solution (Tris-HCl (100 mM, pH 8.5), PEG 8,000 (13%, w/v), glycerol (20%), Tob (40 mM), and CoA (5 mM)), and rapidly frozen in liquid nitrogen.

The X-ray diffraction data were collected at beam line 21ID of the APS at the Argonne National Laboratory at 100 K and processed with HKL2000^[18] (Table 2). The structure was determined by molecular replacement with Phaser^[19] using the Eis hexamer from our previous structure (PDB ID: 3R1K^[5]) as a search model. The structure contained one Eis hexamer per asymmetric unit. After rigid-body and NCS-restrained refinement with Refmac,^[20] six CoAs (one per monomer) were positioned in the difference electronic density, as in our previous structure.^[5] The $F_o - F_c$ map revealed a strong difference density for Tob in two of the six binding sites. Tob could be modeled into this density and refined equally well in either of the two possible conformations, due to the pseudo-symmetry of Tob and data resolution limitations. The structure was refined with three sets of NCS restraints, one for six Eis monomers, one for six CoAs, and one for two Tobs.

Analysis of solvent-accessible surface area (ASA): The ASA calculations for the structure of EisC204A-CoA-Tob complex and structures of other complexes of AG-modifying enzymes with Tob available in the PDB were performed with Surface Racer^[21] (Tables S10 and S11).

Data deposition: The PDB accession code for the structure of EisC204A-CoA-Tob complex is 4JD6.

Acknowledgements

This work was supported by a National Institutes of Health (NIH) Grant AI090048 (S.G.-T.) and a grant from the Firland Foundation (S.G.-T.). J.L.H. was supported by the Cellular Biotechnology Training Program, a Rackham Merit Fellowship, and an American Foundation of Pharmaceutical Education fellowship. We thank Dr. Tomasz Cierpicki (University of Michigan) for assistance with the 600 MHz NMR data collection. We thank the staff of Sector LS-CAT at the Advanced Photon Source (APS) at the Argonne National Laboratory for assistance with the collection of the X-ray diffraction data.

J.H.L. designed and performed all the NMR experiments. W.C. performed TLC experiments, cloned, overexpressed, purified, and analyzed the EisC204A mutant and grew crystals of the EisC204A-CoA-Tob complex. T.B. processed the crystals of the EisC204A-CoA-Tob complex. T.B. and O.V.T. collected X-ray diffraction data and determined the structure of the EisC204A-CoA-Tob

complex. S.G.-T. contributed to the overall study design. J.H.L., O.V.T., and S.G.-T. wrote the manuscript. All authors discussed the results and commented on the manuscript. The authors declare no competing financial interests.

Keywords: bacterial resistance · enhanced intracellular survival protein · enzymatic reaction · multi-acetylation · tuberculosis

- [1] a) M. A. Zaunbrecher, R. D. Sikes, Jr., B. Metchock, T. M. Shinnick, J. E. Posey, *Proc. Natl. Acad. Sci. USA* **2009**, *106*, 20004–20009; b) P. J. Campbell, G. P. Morlock, R. D. Sikes, T. L. Dalton, B. Metchock, A. M. Starks, D. P. Hooks, L. S. Cowan, B. B. Plikaytis, J. E. Posey, *Antimicrob. Agents Chemother.* **2011**, *55*, 2032–2041.
- [2] H. N. Jnawali, H. Yoo, S. Ryoo, K. J. Lee, B. J. Kim, W. J. Koh, C. K. Kim, H. J. Kim, Y. K. Park, *World J. Microbiol. Biotechnol.* **2013**, *29*, 975–982.
- [3] a) W. Chen, K. D. Green, O. V. Tsodikov, S. Garneau-Tsodikova, *Biochemistry* **2012**, *51*, 4959–4967; b) R. E. Pricer, J. L. Houghton, K. D. Green, A. S. Mayhoub, S. Garneau-Tsodikova, *Mol. Biosyst.* **2012**, *8*, 3305–3313.
- [4] a) J. L. Houghton, K. D. Green, R. E. Pricer, A. S. Mayhoub, S. Garneau-Tsodikova, *J. Antimicrob. Chemother.* **2013**, *68*, 800–805; b) K. H. Kim, D. R. An, J. Song, J. Y. Yoon, H. S. Kim, H. J. Yoon, H. N. Im, J. Kim, J. Kim do, S. J. Lee, H. M. Lee, H. J. Kim, E. K. Jo, J. Y. Lee, S. W. Suh, *Proc. Natl. Acad. Sci. USA* **2012**, *109*, 7729–7734.
- [5] W. Chen, T. Biswas, V. R. Porter, O. V. Tsodikov, S. Garneau-Tsodikova, *Proc. Natl. Acad. Sci. USA* **2011**, *108*, 9804–9808.
- [6] K. D. Green, W. Chen, J. L. Houghton, M. Fridman, S. Garneau-Tsodikova, *ChemBioChem* **2010**, *11*, 119–126.
- [7] a) M. W. Vetting, S. S. Hegde, F. Javid-Majid, J. S. Blanchard, S. L. Roderick, *Nat. Struct. Biol.* **2002**, *9*, 653–658; b) K. Shi, D. R. Houston, A. M. Berghuis, *Biochemistry* **2011**, *50*, 6237–6244; c) C. Parthier, S. Gorlich, F. Jaenecke, C. Breithaupt, U. Brauer, U. Fandrich, D. Clausnitzer, U. F. Wehmeier, C. Bottcher, D. Scheel, M. T. Stubbs, *Angew. Chem.* **2012**, *124*, 4122–4128; *Angew. Chem. Int. Ed.* **2012**, *51*, 4046–4052; d) Q. Vicens, E. Westhof, *Chem. Biol.* **2002**, *9*, 747–755.
- [8] S. Fujimura, Y. Tokue, H. Takahashi, T. Nukiwa, K. Hisamichi, T. Mikami, A. Watanabe, *J. Antimicrob. Chemother.* **1998**, *41*, 495–497.
- [9] S. Fujimura, Y. Tokue, H. Takahashi, T. Kobayashi, K. Gomi, T. Abe, T. Nukiwa, A. Watanabe, *FEMS Microbiol. Lett.* **2000**, *190*, 299–303.
- [10] a) J. Kondo, B. Francois, R. J. Russell, J. B. Murray, E. Westhof, *Biochimie* **2006**, *88*, 1027–1031; b) B. Francois, R. J. Russell, J. B. Murray, F. Abouela, B. Masquida, Q. Vicens, E. Westhof, *Nucleic Acids Res.* **2005**, *33*, 5677–5690.
- [11] M. S. Ramirez, M. E. Tolmasky, *Drug Resist. Updates* **2010**, *13*, 151–171.
- [12] J. Kondo, M. Koganei, J. P. Maiani, V. L. Ly, S. Hanessian, *ChemMedChem* **2013**, *8*, 733–739.
- [13] A. Z. Reeves, P. J. Campbell, R. Sultana, S. Malik, M. Murray, B. B. Plikaytis, T. M. Shinnick, J. E. Posey, *Antimicrob. Agents Chemother.* **2013**, *57*, 1857–1865.
- [14] K. D. Green, W. Chen, S. Garneau-Tsodikova, *ChemMedChem* **2012**, *7*, 73–77.
- [15] J. E. Hugonnet, L. W. Tremblay, H. I. Boshoff, C. E. Barry III, J. S. Blanchard, *Science* **2009**, *323*, 1215–1218.
- [16] A. J. Simpson, S. A. Brown, *J. Magn. Reson.* **2005**, *175*, 340–346.
- [17] S. N. Ho, H. D. Hunt, R. M. Horton, J. K. Pullen, L. R. Pease, *Gene* **1989**, *77*, 51–59.
- [18] Z. Otwinowski, W. Minor in *Methods in Enzymology, Macromolecular Crystallography, Part A, Vol. 276* (Ed.: J. R. M. S. C. W. Carter), Academic Press, New York, **1997**, pp. 307–326.
- [19] A. J. McCoy, R. W. Grosse-Kunstleve, P. D. Adams, M. D. Winn, L. C. Storoni, R. J. Read, *J. Appl. Crystallogr.* **2007**, *40*, 658–674.
- [20] G. N. Murshudov, A. A. Vagin, E. J. Dodson, *Acta Crystallogr. Sect. D* **1997**, *53*, 240–255.
- [21] O. V. Tsodikov, M. T. Record, Jr., Y. V. Sergeev, *J. Comput. Chem.* **2002**, *23*, 600–609.
- [22] R. A. Laskowski, M. W. Macarthur, D. S. Moss, J. M. Thornton, *J. Appl. Crystallogr.* **1993**, *26*, 283–291.

Received: June 4, 2013

Published online on September 17, 2013